

# Brain iron content and cognitive function in patients with $\beta$ -thalassemia

Meiru Bu , Xi Deng, Yu Zhang, Sean W. Chen, Muliang Jiang and Bihong T. Chen

*Ther Adv Hematol*

2023, Vol. 14: 1–11

DOI: 10.1177/  
20406207231167050

© The Author(s), 2023.  
Article reuse guidelines:  
[sagepub.com/journals-](https://sagepub.com/journals-permissions)  
permissions

**Abstract:** Patients with  $\beta$ -thalassemia ( $\beta$ -TM) may have brain iron overload from long-term blood transfusions, ineffective erythropoiesis, and increased intestinal iron absorption, leading to cognitive impairment. Brain magnetic resonance imaging (MRI) methods such as the transverse relaxation rate, susceptibility-weighted imaging, and quantitative susceptibility mapping can provide quantitative, *in vivo* measurements of brain iron. This review assessed these MRI methods for brain iron quantification and the measurements for cognitive function in patients with  $\beta$ -TM. We aimed to identify the neural correlates of cognitive impairment, which should help to evaluate therapies for improving cognition and quality of life in patients with  $\beta$ -TM.

**Keywords:**  $\beta$ -thalassemia, brain iron, cognitive function, magnetic resonance imaging

Received: 28 June 2022; revised manuscript accepted: 15 March 2023.

## Introduction

Thalassemia (TM) is a group of disorders caused by defective production of the globin chains of hemoglobin, resulting in chronic anemia with varying severity.<sup>1</sup> TM has a worldwide distribution. In China, regions in the southwest and south have a high incidence of TM, and the Guangdong and Guangxi provinces have the highest incidence.<sup>2</sup> The TM carrier rate for Guangxi province is approximately 24%.<sup>3</sup> TM is classified into five types, that is,  $\alpha$ -,  $\beta$ -,  $\gamma$ -,  $\delta$ -, and  $\delta\beta$ -TM, according to genotyping,<sup>4</sup> and  $\beta$ -TM is the most commonly seen TM in China.<sup>5</sup>  $\beta$ -TM can be divided into minor, intermediate, and major subtypes according to the severity of anemia. Patients with minor  $\beta$ -TM are usually asymptomatic.<sup>6</sup> Patients with major  $\beta$ -TM have symptoms of severe anemia shortly after birth and have life-long dependence on blood transfusion and iron chelation.<sup>7</sup> Currently, the main treatment strategies for the major  $\beta$ -TM include blood transfusion, iron chelation therapy, splenectomy, allogeneic hematopoietic stem cell transplantation, and gene activation therapy.<sup>8</sup>

Long-term blood transfusion, ineffective erythropoiesis, and increased intestinal iron absorption increase the iron load in the body. When the

body's iron metabolism capacity is exceeded, iron overload may occur in multiple organs, resulting in complications such as cardiomyopathy and liver sclerosis, which are well recognized in clinical practice.<sup>8,9</sup> However, the effects of  $\beta$ -TM-related iron overload on the central nervous system are not well known. A landmark 2019 article in the *British Journal of Haematology* recommended that all physicians take cognitive impairment into account when treating transfusion-dependent TM.<sup>10</sup> Other studies have shown that patients with  $\beta$ -TM have brain iron overload, and have proposed a link of brain iron to neurocognitive function.<sup>11–13</sup> However, there is limited knowledge about the neuroanatomical correlates of brain iron deposition, the extent of iron distribution, and its potential association with cognitive impairment. More work needs to be done to identify the neuroimaging biomarkers for cognitive function and to alleviate the neurotoxicity of brain iron overload in patients with  $\beta$ -TM.

Here, we reviewed the magnetic resonance imaging (MRI) methods for brain iron quantification and the measurements for cognitive function in patients with  $\beta$ -TM. We aimed to identify the neural correlates of cognitive impairment, which should help to

Correspondence to:

**Muliang Jiang**  
Department of Radiology,  
First Affiliated Hospital  
of Guangxi Medical  
University, Nanning  
530021, P. R. China.  
[jmlgxmu@gmail.com](mailto:jmlgxmu@gmail.com)

**Meiru Bu**  
**Xi Deng**  
**Yu Zhang**  
Department of Radiology,  
First Affiliated Hospital  
of Guangxi Medical  
University, Nanning, P.  
R. China

**Sean W. Chen**  
Department of Medical  
Oncology & Experimental  
Therapeutics, City of Hope  
Comprehensive Cancer  
Center, Duarte, CA, USA

**Bihong T. Chen**  
Department of Diagnostic  
Radiology, City of Hope  
National Medical Center,  
Duarte, CA, USA

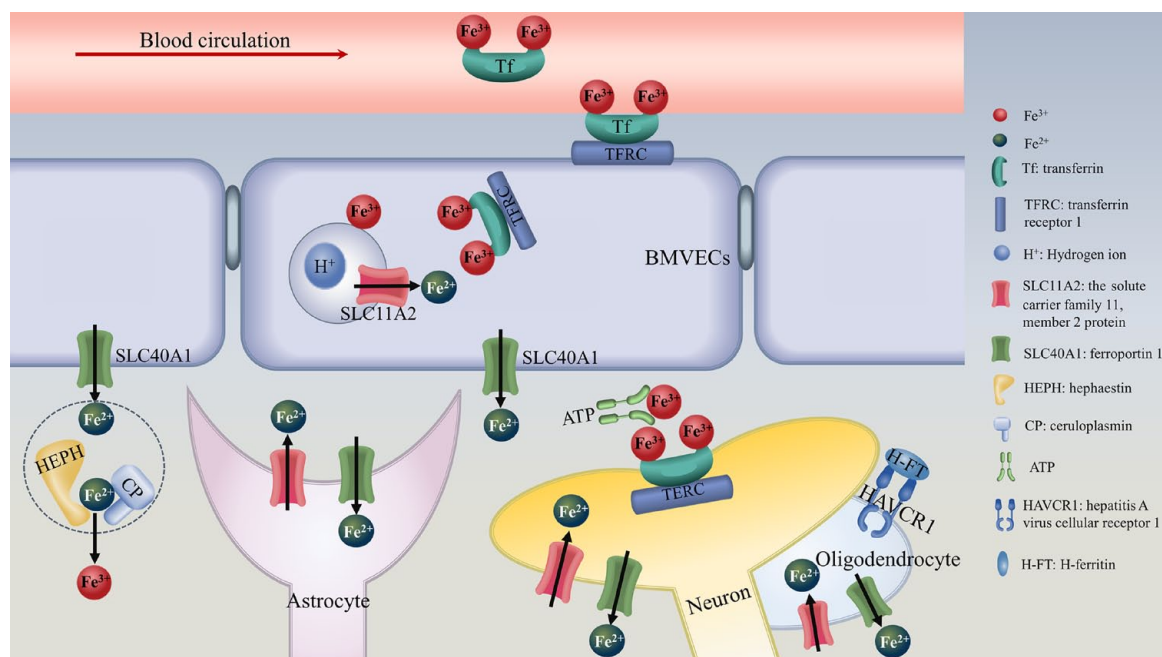


**Figure 1.** Brain iron transport and metabolism. CP, ceruloplasmin; HAVCR1=TIM-1, hepatitis A virus cellular receptor 1; HEPH, hephaestin; H-FT, H-ferritin; SLC11A2=DMT1, the solute carrier family 11, member 2 protein; SLC40A1=FPN1 ferroportin 1; Tf, transferrin; TFRC, transferrin receptor 1.

evaluate therapies for improving cognition and quality of life in patients with  $\beta$ -TM.

### Brain iron metabolism

Iron is the most abundant metal in the brain,<sup>14</sup> and it plays a role in pleiotropic functions including oxidative metabolism, myelin production, neurotransmitter synthesis and other biophysiological processes in the central nervous system.<sup>15</sup> Iron travels from the peripheral blood circulation into the brain mainly by crossing the blood–brain barrier, which consists of brain microvascular endothelial cells (BMVECs), pericytes, and basement membrane.<sup>16</sup> Serum ferritin level is not equivalent to brain ferritin level. Specifically, iron binds the transferrin (Tf-Fe) in the blood, and Tf-Fe binds to the transferrin receptor 1 (TFRC, also known as TfR1) in BMVECs. The BMVECs then form endosomes after endocytosis of Tf-TFRC.<sup>17</sup> When the endosomal pH is decreased to 5.5~6.5, ferric iron ( $\text{Fe}^{3+}$ ) is reverted to ferrous iron ( $\text{Fe}^{2+}$ ), which releases from the endosomes into the endothelial cytoplasm with the help of the solute carrier family 11, member 2 protein (SLC11A2, also known as DMT1).<sup>18</sup> Intracellular  $\text{Fe}^{2+}$  is exported from the BMVECs

by ferroportin (SLC40A1, also known as FPN1) and is oxidized to  $\text{Fe}^{3+}$  with the help of ceruloplasmin (CP) or hephaestin (HEPH).<sup>19</sup> After iron enters the brain interstitial fluid, it is taken up by multiple types of cells in various brain regions.<sup>18</sup> Neurons can take up Tf-Fe via TFRC due to the widespread distribution of TFRC.<sup>20</sup> There is also a SLC11A2-dependent transport mechanism for  $\text{Fe}^{2+}$  in neurons, astrocytes, and oligodendrocytes.<sup>21</sup> Recent studies show that oligodendrocytes can acquire iron via the hepatitis A virus cellular receptor 1 (HAVCR1, also known as TIM-1) protein, a ferritin receptor expressed in oligodendrocytes, which binds H-ferritin.<sup>19,20,22</sup> The process of brain iron transport and metabolism process is presented in Figure 1.

### MRI methods for brain iron quantification

MRI can quantitatively assess the location and composition of brain iron deposits *in vivo*. Brain iron is primarily stored as non-heme iron, such as ferritin and hemosiderin, and is distributed unevenly in the brain, with higher concentrations in the basal ganglia, substantia nigra, and red nucleus; lower concentrations in the gray matter regions; and the lowest concentration in

**Table 1.** Quantitative magnetic resonance imaging methods for brain iron measurement.

Methods	References	Subjects	Regions with brain iron overload
R2	Barbosa <i>et al.</i> <sup>26</sup>	20 patients with Parkinson disease, 30 healthy controls	Substantia nigra, red nucleus, caudate nucleus, globus pallidus, putamen, thalamus
	Uddin <i>et al.</i> <sup>27</sup>	17 healthy adults	Globus pallidus, substantia nigra, red nucleus, putamen, thalamus, caudate nucleus, cortical gray matter
R2'	Sedlacik <i>et al.</i> <sup>28</sup>	66 healthy adults	Globus pallidus, putamen, caudate nucleus, hippocampus, amygdala, motor cortex
	Balasubramanian <i>et al.</i> <sup>29</sup>	18 healthy adults	Globus pallidus, thalamus, putamen
	Larsen <i>et al.</i> <sup>30</sup>	146 adolescents and young adults	Caudate nucleus, putamen, nucleus accumbens
R2*	Cler <i>et al.</i> <sup>31</sup>	41 adults who stutter; 32 adults who are typically fluent	Left putamen, left frontal operculum and insula
	Elalfy <i>et al.</i> <sup>32</sup>	32 patients with sickle cell disease; 15 patients with $\beta$ -TM; 11 healthy controls	Thalamus, caudate nucleus
	Raab <i>et al.</i> <sup>24</sup>	74 healthy children	Globus pallidus, caudate nucleus, putamen
SWI	Park <i>et al.</i> <sup>33</sup>	127 patients with Alzheimer disease; 127 healthy controls	Motor cortex, sensory cortex, medial frontal cortex
	Xiong <i>et al.</i> <sup>34</sup>	17 patients with Parkinson disease; 10 healthy controls	Substantia nigra, red nucleus, globus pallidus, thalamus, putamen, caudate nucleus, dentate nucleus
	Khattar <i>et al.</i> <sup>35</sup>	92 healthy adults	Globus pallidus, red nucleus, putamen, caudate nucleus, amygdala, hippocampus, insula, substantia nigra
QSM	Thomas <i>et al.</i> <sup>36</sup>	100 patients with Parkinson disease; 37 healthy controls	Prefrontal cortex, putamen, hippocampus, thalamus, caudate nucleus, substantia nigra
	Li <i>et al.</i> <sup>37</sup>	23 patients with type 2 diabetes; 25 healthy controls	Right caudate nucleus, putamen, globus pallidus, frontal inferior triangular gyrus, and precentral gyrus
	Howard <i>et al.</i> <sup>38</sup>	67 healthy adults	Right inferior temporal gyrus, bilateral putamen, posterior cingulate gyrus, motor, and premotor cortices
	Chen <i>et al.</i> <sup>39</sup>	150 cognitively normal older adults	Hippocampus, putamen, globus pallidus, caudate nucleus, entorhinal cortex, frontal cortex, temporal cortex

$\beta$ -TM, beta-thalassemia; QSM, quantitative susceptibility mapping; SWI, susceptibility-weighted imaging.

the white matter.<sup>23–25</sup> MRI quantifies the ferritin and hemosiderin signal, thus reflecting the brain iron deposition. Several MRI techniques have been used to quantify iron levels, including the transverse relaxation rate (R2, R2',

R2\*), susceptibility-weighted imaging (SWI) and quantitative susceptibility mapping (QSM), as presented in Table 1. The strengths and limitations of each technique will be described in the following sections.

#### *Transverse relaxation rate (R2, R2', R2\*)*

As a paramagnetic substance, ferritin creates inhomogeneity in a local magnetic field, which shortens the transverse relaxation time of protons (T2) and increases the transverse relaxation rate ( $R2 = 1/T2$ ).<sup>40</sup> Prior studies have shown that the R2 values of deep gray matter nuclei such as the globus pallidus, putamen, caudate nucleus, and thalamus are positively correlated with iron content in healthy adults.<sup>27</sup> A postmortem study showed a strong linear correlation between R2 values and brain iron concentrations, with the highest iron concentrations noted in the globus pallidus, followed by the putamen, caudate nucleus, and thalamus.<sup>41</sup> However, the water content of brain tissue could increase the R2 value, which could affect the determination of gray matter iron content.<sup>40</sup> Consequently, the R2 method is not specific for iron quantification in the gray matter.

The reversible transverse relaxation rate ( $R2' = 1/T2'$ ) reflects the reversible signal losses associated with local magnetic field inhomogeneity, which can eliminate the confounding effects of water content in brain tissue.<sup>40</sup> A study of young, middle-aged, and older people showed that the iron concentrations in the globus pallidus and putamen, measured as R2', positively correlate with age.<sup>42</sup> Despite its specificity for measuring the deep gray matter iron content,<sup>27,28</sup> R2' has limitations due to low image resolution and cumbersome calculation, which requires the removal of background fields to achieve local field inhomogeneity.<sup>42</sup>

According to MRI relaxation theory, the effective transverse relaxation rate  $R2^* = R2 + R2'$ , where  $R2^* = 1/T2^*$ ,  $R2 = 1/T2$ , and  $R2' = 1/T2'$ .<sup>42</sup> The R2\* value is obtained using a single exponential to fit multi-echo amplitude signals in the gradient echo sequence, which can quantitatively analyze the iron content in the tissue.<sup>43</sup> A prior study demonstrated that the R2\* value of the left putamen, left frontal operculum, and insula in individuals who stutter is higher than in those who are typically fluent, and the higher R2\* values in these brain regions indicates higher brain iron levels.<sup>31</sup> However, R2\* can detect a spurious signal at the junctions of tissues with large differences in susceptibility, which reflects an overall change in magnetic sensitivity. Also, it does not precisely detect the concentration of brain iron because

ongoing myelination in the brain can increase the R2\* value.<sup>24</sup>

#### *Susceptibility-weighted imaging*

SWI is an innovative MRI technique that takes advantage of differential magnetic sensitivity in tissue to enhance imaging contrast. SWI can also enhance susceptibility contrast using the phase values obtained in gradient echo imaging.<sup>44</sup> Ferritin as a highly paramagnetic substance can induce changes in local magnetic field, cause proton dephasing, and result in low signal on the phase images.<sup>45</sup> A study using SWI to assess brain iron levels in healthy adults ranging from 21 to 94 years of age showed that brain iron content was linearly correlated with age and had a negative association with myelin content.<sup>35</sup> Although the phase value measured on SWI can indirectly reflect the iron content, the phase images generated from SWI depend on the orientation of structures relative to the applied magnetic field. In addition, SWI cannot measure the susceptibility of each voxel locally,<sup>25</sup> which may affect the accuracy of the phase value which reflects the brain iron content.

#### *Quantitative susceptibility mapping*

The susceptibility of a substance to an external magnetic field is a unique characteristic. QSM provides quantitative estimates of local magnetic susceptibility at a voxel level by solving a complex field-to-source inversion issue and this method quantifies *in vivo* brain iron levels accurately.<sup>46</sup> One study of brain iron content in mouse iron overload models showed that QSM provided more accurate and sensitive detection of brain iron deposition than R2\*.<sup>43</sup> A study of Parkinson disease (PD) demonstrated that a QSM-derived measure of brain iron content increased in the hippocampus, thalamus, and caudate nucleus in patients with PD, compared with controls without PD, and QSM-derived brain iron content was negatively correlated with cognitive function.<sup>36</sup> QSM is a sensitive technique for detecting brain iron content, but it is susceptible to interference from the white matter myelin, and increased susceptibility can be caused by increased iron, decreased myelin (demyelination), or both.<sup>47</sup> Therefore, combining R2\* and QSM may optimize evaluation of iron and myelination-induced susceptibility changes.<sup>46</sup>

Among the commonly used MRI methods for brain iron quantification, QSM is currently the most accurate method for determining brain iron content *in vivo*. Since R2 has a low specificity and cannot fully eliminate the confounding effect of water in the brain tissue, it has been used less frequently to measure brain iron content. On the contrary, R2' can eliminate these confounding effects, and it has high specificity for iron content in deep gray matter. Nevertheless, considering the complexity in data processing, cumbersome calculations, and low image resolution, it is not used frequently either. The method with R2\* reflects both brain iron and myelin content, meaning that changes in the myelin content of the brain in addition to iron would also increase the R2\* value. Therefore, more studies combine R2\* and QSM to quantitate brain iron content,<sup>24,47–49</sup> since these two methods provide complementary information, that is, iron increases both R2\* and QSM, while myelin elevates R2\* but decreases QSM.

### Cognitive function in patients with $\beta$ -TM

With the advancement of therapies such as iron chelation therapy, the life expectancy of patients with  $\beta$ -TM has increased significantly.<sup>50</sup> Iron chelation improves cognitive function in TM patients because it prevents and treats complications such as cardiac and liver sclerosis by removing excess iron, thus improving quality of life in patients with TM.<sup>51</sup> A recent study showed that a lack of iron chelation therapy was an independent factor associated with cognitive impairment in patients with TM.<sup>52</sup> The increase in life expectancy has motivated the medical community to focus more on improving the cognitive function and quality of life of patients with  $\beta$ -TM. As a result, the neurological complications of  $\beta$ -TM are gradually being recognized. Most of these neurological complications are subclinical and are detected only in neuropsychological tests, neuroelectrophysiological tests, or neuroimaging.<sup>53,54</sup> It is noteworthy that patients with  $\beta$ -TM who require medical attention are mainly of school-age, and cognitive impairments such as learning and memory issues are major concerns for this population.

### Neuropsychological findings

Patients with  $\beta$ -TM show various cognitive deficits. For instance, Economou *et al.*<sup>55</sup> showed that

36.36% of patients with  $\beta$ -TM have an abnormal total intelligence quotient (IQ) score compared with healthy children, as assessed by the Wechsler Intelligence Scale for Children–Third Edition. Another study found that the  $\beta$ -TM group had lower full-scale, performance, and verbal IQ scores when compared with the healthy control group, using the Turkish version of the Wechsler Intelligence Scale for Children-Revised.<sup>56</sup> Additional studies have identified lower full-scale and/or performance IQ scores in patients with  $\beta$ -TM compared with controls.<sup>13,57,58</sup> In terms of memory and attention, Monastero *et al.*<sup>11</sup> found significant differences in verbal memory and attention between patients and controls using the Wechsler Adult Intelligence Scale (WAIS) Digit Span and Trail Making Test. In addition, using the California Verbal Learning Test and WAIS Digit Span test, Daar *et al.*<sup>59</sup> showed that short-term memory capacity, as well as verbal and auditory attention, was impaired in patients with  $\beta$ -TM compared with controls. Regarding executive function, Elalfy *et al.*<sup>60</sup> found the percentage of perseverative errors on the Wisconsin Card Sorting Test was higher in  $\beta$ -TM patients compared with controls, implicating executive dysfunction in these patients. Furthermore, Daar *et al.*<sup>59</sup> showed that patients with  $\beta$ -TM had lower verbal fluency scores as compared with healthy controls when assessed with the Controlled Oral Word Association Test. Studies have shown more cognitive impairment in patients with transfusion-dependent TM compared with patients who were not transfusion-dependent.<sup>52,61</sup> Several factors may contribute to impaired cognition in patients with transfusion dependence, including brain iron overload due to long-term transfusion, chronic hypoxia caused by severe anemia, and toxicity associated with iron chelation drugs.<sup>54</sup>

A study by Ahmadpanah *et al.*<sup>62</sup> showed no significant differences in executive function, attention, and working memory in patients with  $\beta$ -TM compared with controls. Their result might be partially explained by the small sample size and inclusion of subjects with  $\beta$ -TM minor who did not need blood transfusion therapy or iron chelation and hence had a lower risk for cognitive impairment. Also, although neuropsychological testing is the gold standard for evaluating cognitive function in patients with  $\beta$ -TM, there are various neuropsychological testing batteries with different sensitivities and are validated with

different measures. These testing batteries could be affected by the education and cultural background of the patients and subjective factors of the people who performed the assessment.<sup>63</sup> Therefore, other methods are needed to assess the extent of cognitive impairment objectively in patients with  $\beta$ -TM. Furthermore, a link between brain iron and cognition has not been clearly identified in patients with  $\beta$ -TM. Other factors such as missed days at school, time spent in the hospital, recurrent anemia, diminished quality of life and decreased life expectancy may have an impact on cognition in patients with  $\beta$ -TM.

#### Neuro-electrophysiological findings

Event-related potentials (ERPs) provide a non-invasive neuro-electrophysiological method for evaluating the central nervous system with excellent temporal resolution. ERPs can be divided into various components according to the waveform.<sup>64</sup> For instance, the P300 wave reflects the speed of neuronal events during stimulus processing and can be used to assess the information processing function of the brain.<sup>65</sup> Nevruz *et al.*<sup>66</sup> examined P300 waves during an auditory discrimination task in children with  $\beta$ -TM minor and healthy controls. They found that patients had a prolonged latency and reduced amplitude of P300 waves compared with the controls. Interestingly, Shehata *et al.*<sup>67</sup> and Elalfy *et al.*<sup>60</sup> also observed prolonged latency and reduced amplitude of P300 waves in patients with  $\beta$ -TM major. In another ERP study of patients with  $\beta$ -TM, Raz *et al.*<sup>68</sup> found a longer response time compared with controls. Moreover, they showed that hemoglobin levels were negatively correlated with the amplitudes of the ERP components, as the lower the hemoglobin levels, the greater the amplitudes of the P2, N1, N2, and P300 waves. The main advantage of the ERP method is to allow various cognitive components to be extracted at each stage of cognitive processing.<sup>69</sup> However, there are limitations to the ERP method, including the low spatial resolution of ERPs<sup>70</sup> and the variability in indicators, such as latency and amplitude, among subjects.<sup>71</sup> It is therefore prudent to use ERP in combination with other methods to improve its specificity. For instance, the neuropsychological testing and MRI methods are commonly paired with ERP.<sup>60,65</sup>

#### Neuroimaging findings

Cognitive impairment in  $\beta$ -TM patients has been attributed to various factors, such as iron overload, chronic hypoxia, and deferoxamine neurotoxicity.<sup>64,65,72</sup> More recently, it has been shown that brain iron overload can induce oxidative stress via the Fenton reaction, which results in irreversible brain damage through ferroptosis of neurons and neuroglial cells. This process may be an important mechanism underlying cognitive impairment in  $\beta$ -TM patients.<sup>73</sup> Animal studies have shown an association between cognitive dysfunction and brain iron overload in the mouse model of Alzheimer disease.<sup>74,75</sup> An iron overload model of nursing piglets showed an association between hippocampus iron overload and impaired social novelty recognition.<sup>76</sup> In addition, human studies in patients with non- $\beta$ -TM and cognitive impairment have demonstrated that brain iron deposition is correlated with cognitive impairment.<sup>77-79</sup> Currently, MRI is the most commonly used neuroimaging method for quantification of brain iron content *in vivo*, making it a crucial technique for evaluating brain iron overload in patients with  $\beta$ -TM. The key neuroimaging findings of brain iron accumulation in patients with  $\beta$ -TM with or without cognitive assessment are presented in Table 2.

The studies by Tartaglione *et al.*<sup>61</sup> and Manara *et al.*<sup>82</sup> on the same study group showed cognitive impairment in patients with  $\beta$ -TM when compared with controls. However, their studies showed no iron overload in the brain tissue but in the choroid plexuses, and there was no correlation between cognitive impairment and brain iron overload in patients with  $\beta$ -TM. A potential explanation might be due to their using R2\* to measure brain iron and a high R2\* value may not be specific to increase in iron since R2\* reflects both iron and myelin content.

To date, there is no consensus on the specific brain regions where iron accumulates in patients with  $\beta$ -TM. Prior studies by Qiu *et al.*,<sup>81</sup> Manara *et al.*,<sup>82</sup> and Witzleben *et al.*<sup>83</sup> indicated that brain iron accumulated almost exclusively in the choroid plexus in patients with  $\beta$ -TM. The study by Qiu *et al.*<sup>81</sup> also showed iron increase in the red nucleus in addition to choroid plexus. However, no studies have found any association between iron overload and cognitive impairment. Therefore, it remains largely unknown whether

**Table 2.** Neuroimaging findings of brain iron overload in patients with beta-thalassemia.

References	Subjects	MRI method	Regions of brain iron overload	Assessment of cognitive function	Correlation of brain iron and cognitive function
Metafratzi <i>et al.</i> <sup>12</sup>	41 patients with $\beta$ -TM; 58 healthy controls	R2 (1.5TMRI)	Putamen, caudate nucleus, motor cortex, temporal cortex	None	
Akhlaghpoor <i>et al.</i> <sup>80</sup>	53 patients with $\beta$ -TM; 40 healthy controls	T2* (1.5TMRI)	Basal ganglia (striatum), thalamus	None	
Qiu <i>et al.</i> <sup>81</sup>	31 patients with $\beta$ -TM; 33 healthy controls	QSM (3TMRI)	Choroid plexus, red nucleus	None	
Tartaglione <i>et al.</i> <sup>61</sup>	74 patients with $\beta$ -TM; 45 healthy controls	R2* (3TMRI)	Hippocampal formations and around the Luschka foramina, choroid plexuses <sup>a</sup>	WAIS-4th Edition, lower values of full-scale IQ and VCI, PRI, WMI domain in $\beta$ -TM patients compared with controls; BPRS, higher score in $\beta$ -TM patients compared with controls	No correlation between brain iron and WAIS score
Manara <i>et al.</i> <sup>82</sup>	70 patients with $\beta$ -TM; 57 healthy controls	R2* (3TMRI)	Hippocampal formations and around the Luschka foramina, choroid plexuses	WAIS-4th Edition, lower IQ values in $\beta$ -TM patients compared with controls	No correlation between brain iron and WAIS score.
Elalfy <i>et al.</i> <sup>32</sup>	32 patients with sickle cell disease; 15 patients with $\beta$ -TM	R2* (1.5TMRI)	Left thalamus	None	

<sup>1</sup>5TMRI, 1.5 Tesla MRI; 3TMRI, 3 Tesla MRI; BPRS, Brief Psychiatric Rating Scale; IQ, intelligence quotient; MRI, magnetic resonance imaging; PRI, perceptual reasoning index; QSM, quantitative susceptibility mapping; SWI, susceptibility-weighted imaging; VCI, verbal comprehension index; WAIS, Wechsler Adult Intelligence Scale; WMI, working memory index;  $\beta$ -TM, beta-thalassemia.

<sup>a</sup>The two studies of Tartaglione *et al.*<sup>61</sup> and Manara *et al.*<sup>82</sup> from the same study group.

brain iron overload is directly linked to cognitive functioning in patients with  $\beta$ -TM. Furthermore, few studies of brain iron content are conducted in children with  $\beta$ -TM, which has made it challenging to assess for possible association between brain iron overload and cognitive impairment in this vulnerable population.

### Conclusion

MRI methods can be used to study the potential association of brain iron deposition and cognitive function in patients with  $\beta$ -TM. QSM provides a novel, noninvasive, and quantitative method to analyze brain iron. Going forward, it will be important to determine to what extent and how

brain iron overload affects cognitive function in patients with  $\beta$ -TM by combining MRI techniques, neuropsychological tests, and neuro-electrophysiological methods. More research is needed to elucidate the mechanism underlying the cognitive impairment and thus to mitigate the neurotoxicity of brain iron overload in patients with  $\beta$ -TM.

### Declarations

*Ethics approval and consent to participate*

Not applicable.

*Consent for publication*

Not applicable.

#### Author contributions

**Meiru Bu:** Writing – original draft.

**Xi Deng:** Writing – original draft.

**Yu Zhang:** Visualization.

**Sean W. Chen:** Writing – review & editing.

**Muliang Jiang:** Conceptualization, Writing – review & editing.

**Bihong T Chen:** Writing – review & editing.

#### Acknowledgements

The authors would like to thank Nancy Linford, PhD, who provided editing services.

#### Funding

The authors disclosed receipt of the following financial support for the research, authorship, and/or publication of this article: This work was supported by National Natural Science Foundation of China (82260344), Youth Science Foundation of Guangxi Medical University (GXMUYSF202216), P. R. China and ‘Medical Excellence Award’ Funded by the Creative Research Development Grant from the First Affiliated Hospital of Guangxi Medical University, P. R. China.

#### Competing interests

The authors declared no potential conflicts of interest with respect to the research, authorship, and/or publication of this article.

#### Availability of data and materials

Not applicable.

#### ORCID iD

Meiru Bu  <https://orcid.org/0000-0001-8077-6287>

#### References

1. Bajwa H and Basit H. *Thalassemia*. Treasure Island, FL: StatPearls Publishing, 2021.
2. Lai K, Huang G, Su L, *et al*. The prevalence of thalassemia in mainland China: evidence from epidemiological surveys. *Sci Rep* 2017; 7: 920.
3. He S, Qin Q, Yi S, *et al*. Prevalence and genetic analysis of  $\alpha$ - and  $\beta$ -thalassemia in Baise region, a multi-ethnic region in southern China. *Gene* 2017; 619: 71–75.
4. De Simone G, Quattrocchi A, Mancini B, *et al*. Thalassemias: from gene to therapy. *Mol Aspects Med* 2022; 84: 101028.
5. Shang X, Wu X, Zhang X, *et al*. Clinical practice guidelines for beta-thalassemia. *Zhonghua Yi Xue Yi Chuan Xue Za Zhi* 2020; 37: 243–251.
6. Choudhry VP. Thalassemia minor and major: current management. *Indian J Pediatr* 2017; 84: 607–611.
7. Khandros E and Kwiatkowski JL. Beta thalassemia: monitoring and new treatment approaches. *Hematol Oncol Clin North Am* 2019; 33: 339–353.
8. Taher AT, Weatherall DJ and Cappellini MD. Thalassaemia. *Lancet* 2018; 391: 155–167.
9. Cappellini MD, Porter JB, Viprakasit V, *et al*. A paradigm shift on beta-thalassaemia treatment: how will we manage this old disease with new therapies. *Blood Rev* 2018; 32: 300–311.
10. Rund D. Cognition in thalassaemia: the next milestone. *Br J Haematol* 2019; 186: 511–512.
11. Monastero R, Monastero G, Ciaccio C, *et al*. Cognitive deficits in beta-thalassemia major. *Acta Neurol Scand* 2000; 102: 162–168.
12. Metafratzi Z, Argyropoulou MI, Kiortsis DN, *et al*. T(2) relaxation rate of basal ganglia and cortex in patients with beta-thalassaemia major. *Br J Radiol* 2001; 74: 407–410.
13. El-Alameey IR, Alzaree F, Shehata MA, *et al*. Neurocognitive function and its related potentials in children with beta thalassemia major: an Egyptian study. *Open Access Maced J Med Sci* 2019; 7: 322–328.
14. Ashraf A, Clark M and So PW. The aging of iron man. *Front Aging Neurosci* 2018; 10: 65.
15. D’Mello SR and Kindy MC. Overdosing on iron: elevated iron and degenerative brain disorders. *Exp Biol Med* 2020; 245: 1444–1473.
16. Segarra M, Aburto MR and Acker-Palmer A. Blood-brain barrier dynamics to maintain brain homeostasis. *Trends Neurosci* 2021; 44: 393–405.
17. Thirupathi A and Chang YZ. Brain iron metabolism and CNS diseases. *Adv Exp Med Biol* 2019; 1173: 1–19.
18. Yu P and Chang YZ. Brain iron metabolism and regulation. *Adv Exp Med Biol* 2019; 1173: 33–44.
19. Grubić Kezele T and Čurko-Cofek B. Age-related changes and sex-related differences in brain iron metabolism. *Nutrients* 2020; 12: 2601.

20. Qian ZM and Ke Y. Brain iron transport. *Biol Rev Camb Philos Soc* 2019; 94: 1672–1684.
21. Yan N and Zhang J. Iron metabolism, ferroptosis, and the links with Alzheimer's disease. *Front Neurosci* 2019; 13: 1443.
22. Chiou B, Lucassen E, Sather M, *et al.* Semaphorin4A and H-ferritin utilize Tim-1 on human oligodendrocytes: a novel neuro-immune axis. *Glia* 2018; 66: 1317–1330.
23. Ward RJ, Zucca FA, Duyn JH, *et al.* The role of iron in brain ageing and neurodegenerative disorders. *Lancet Neurol* 2014; 13: 1045–1060.
24. Raab P, Ropele S, Bültmann E, *et al.* Analysis of deep grey nuclei susceptibility in early childhood: a quantitative susceptibility mapping and R2\* study at 3 Tesla. *Neuroradiology* 2022; 64: 1021–1031.
25. Sotoudeh H, Sarrami AH, Wang JX, *et al.* Susceptibility-weighted imaging in neurodegenerative disorders: a review. *J Neuroimaging* 2021; 31: 459–470.
26. Barbosa JH, Santos AC, Tumas V, *et al.* Quantifying brain iron deposition in patients with Parkinson's disease using quantitative susceptibility mapping, R2 and R2. *Magn Reson Imaging* 2015; 33: 559–565.
27. Uddin MN, Lebel RM and Wilman AH. Value of transverse relaxometry difference methods for iron in human brain. *Magn Reson Imaging* 2016; 34: 51–59.
28. Sedlacik J, Boelmans K, Löbel U, *et al.* Reversible, irreversible and effective transverse relaxation rates in normal aging brain at 3T. *Neuroimage* 2014; 84: 1032–1041.
29. Balasubramanian M, Polimeni JR and Mulkern RV. In vivo measurements of irreversible and reversible transverse relaxation rates in human basal ganglia at 7 T: making inferences about the microscopic and mesoscopic structure of iron and calcification deposits. *NMR Biomed* 2019; 32: e4140.
30. Larsen B, Olafsson V, Calabro F, *et al.* Maturation of the human striatal dopamine system revealed by PET and quantitative MRI. *Nat Commun* 2020; 11: 846.
31. Cler GJ, Krishnan S, Papp D, *et al.* Elevated iron concentration in putamen and cortical speech motor network in developmental stuttering. *Brain* 2021; 144: 2979–2984.
32. Elalfy MS, Ibrahim AS, Ibrahim GS, *et al.* Hidden brain iron content in sickle cell disease: impact on neurocognitive functions. *Eur J Pediatr* 2021; 180: 2677–2686.
33. Park M, Moon Y, Han SH, *et al.* Motor cortex hypointensity on susceptibility-weighted imaging: a potential imaging marker of iron accumulation in patients with cognitive impairment. *Neuroradiology* 2019; 61: 675–683.
34. Xiong W, Li LF, Huang L, *et al.* Different iron deposition patterns in akinetic/rigid-dominant and tremor-dominant Parkinson's disease. *Clin Neurol Neurosurg* 2020; 198: 106181.
35. Khattar N, Triebswetter C, Kiely M, *et al.* Investigation of the association between cerebral iron content and myelin content in normative aging using quantitative magnetic resonance neuroimaging. *Neuroimage* 2021; 239: 118267.
36. Thomas GEC, Leyland LA, Schrag AE, *et al.* Brain iron deposition is linked with cognitive severity in Parkinson's disease. *J Neurol Neurosurg Psychiatry* 2020; 91: 418–425.
37. Li J, Zhang Q, Zhang N, *et al.* Increased brain iron detection by voxel-based quantitative susceptibility mapping in type 2 diabetes mellitus patients with an executive function decline. *Front Neurosci* 2020; 14: 606182.
38. Howard CM, Jain S, Cook AD, *et al.* Cortical iron mediates age-related decline in fluid cognition. *Hum Brain Mapp* 2021; 43: 1047–1060.
39. Chen L, Soldan A, Oishi K, *et al.* Quantitative susceptibility mapping of brain iron and  $\beta$ -amyloid in MRI and PET relating to cognitive performance in cognitively normal older adults. *Radiology* 2021; 298: 353–362.
40. Haacke EM, Cheng NY, House MJ, *et al.* Imaging iron stores in the brain using magnetic resonance imaging. *Magn Reson Imaging* 2005; 23: 1–25.
41. Langkammer C, Krebs N, Goessler W, *et al.* Quantitative MR imaging of brain iron: a postmortem validation study. *Radiology* 2010; 257: 455–462.
42. Yan F, He N, Lin H, *et al.* Iron deposition quantification: applications in the brain and liver. *J Magn Reson Imaging* 2018; 48: 301–317.
43. Guan JJ and Feng YQ. Quantitative magnetic resonance imaging of brain iron deposition: comparison between quantitative susceptibility mapping and transverse relaxation rate (R2\*) mapping. *Nan Fang Yi Ke Da Xue Xue Bao* 2018; 38: 305–311.
44. Haller S, Haacke EM, Thurnher MM, *et al.* Susceptibility-weighted imaging: technical essentials and clinical neurologic applications. *Radiology* 2021; 299: 3–26.

45. Jeon BU, Yu IK, Kim TK, *et al.* Susceptibility-weighted imaging as a distinctive imaging technique for providing complementary information for precise diagnosis of neurologic disorder. *Taehan Yongsang Uihakhoe Chi* 2021; 82: 99–115.
46. Ravanfar P, Loi SM, Syeda WT, *et al.* Systematic review: quantitative susceptibility mapping (QSM) of brain iron profile in neurodegenerative diseases. *Front Neurosci* 2021; 15: 618435.
47. Treit S, Naji N, Seres P, *et al.* R2\* and quantitative susceptibility mapping in deep gray matter of 498 healthy controls from 5 to 90 years. *Hum Brain Mapp* 2021; 42: 4597–4610.
48. De Barros A, Arribarat G, Lotterie JA, *et al.* Iron distribution in the lentiform nucleus: a post-mortem MRI and histology study. *Brain Struct Funct* 2021; 226: 351–364.
49. Xu M, Guo Y, Cheng J, *et al.* Brain iron assessment in patients with first-episode schizophrenia using quantitative susceptibility mapping. *Neuroimage Clin* 2021; 31: 102736.
50. Origa R.  $\beta$ -thalassemia. *Genet Med* 2017; 19: 609–619.
51. Pinto VM and Forni GL. Management of iron overload in beta-thalassemia patients: clinical practice update based on case series. *Int J Mol Sci* 2020; 21: 8771.
52. Limpawattana P, Juntararungtong T, Teawtrakul N, *et al.* Cognitive impairment in thalassemia and associated factors. *Dement Geriatr Cogn Disord* 2022; 51: 128–134.
53. Rund D and Rachmilewitz E. New trends in the treatment of  $\beta$ -thalassemia. *Crit Rev Oncol Hematol* 2000; 33: 105–118.
54. Nemtsas P, Arnaoutoglou M, Perifanis V, *et al.* Neurological complications of beta-thalassemia. *Ann Hematol* 2015; 94: 1261–1265.
55. Economou M, Zafeiriou DI, Kontopoulos E, *et al.* Neurophysiologic and intellectual evaluation of beta-thalassemia patients. *Brain Dev* 2006; 28: 14–18.
56. Duman O, Arayici S, Fettahoglu C, *et al.* Neurocognitive function in patients with  $\beta$ -thalassemia major. *Pediatr Int* 2011; 53: 519–523.
57. Raafat N, El Safy U, Khater N, *et al.* Assessment of cognitive function in children with beta-thalassemia major: a cross-sectional study. *J Child Neurol* 2015; 30: 417–422.
58. Raz S, Koren A, Dan O, *et al.* Cognitive functions in adults with  $\beta$ -thalassemia major: before and after blood transfusion and comparison with healthy controls. *Ann N Y Acad Sci* 2016; 1375: 19–27.
59. Daar S, Al Saadoon M, Wali Y, *et al.* Cognitive function in adults with beta-thalassemia major in Oman: a pilot study. *Oman Med J* 2021; 36: e322.
60. Elalfy MS, Aly RH, Azzam H, *et al.* Neurocognitive dysfunction in children with  $\beta$  thalassemia major: psychometric, neurophysiologic and radiologic evaluation. *Hematology* 2017; 22: 617–622.
61. Tartaglione I, Manara R, Caiazza M, *et al.* Brain functional impairment in beta-thalassaemia: the cognitive profile in Italian neurologically asymptomatic adult patients in comparison to the reported literature. *Br J Haematol* 2019; 186: 592–607.
62. Ahmadpanah M, Asadi Y, Haghghi M, *et al.* In patients with minor beta-thalassemia, cognitive performance is related to length of education, but not to minor beta-thalassemia or hemoglobin levels. *Iran J Psychiatry* 2019; 14: 47–53.
63. Howieson D. Current limitations of neuropsychological tests and assessment procedures. *Clin Neuropsychol* 2019; 33: 200–208.
64. Azevedo AA, Figueiredo RR and Penido NO. Tinnitus and event related potentials: a systematic review. *Braz J Otorhinolaryngol* 2020; 86: 119–126.
65. Raz S, Koren A, Dan O, *et al.* Executive function and neural activation in adults with  $\beta$ -thalassemia major: an event-related potentials study. *Ann N Y Acad Sci* 2016; 1386: 16–29.
66. Nevruz O, Ulas U, Cetin T, *et al.* Cognitive dysfunction in beta-thalassemia minor. *Am J Hematol* 2007; 82: 203–207.
67. Shehata GA, Elsayh KI, Rafet NH, *et al.* Study of  $\beta$ -thalassemia biomarkers and their relationship to cognition among children. *J Child Neurol* 2010; 25: 1473–1479.
68. Raz S, Koren A and Levin C. Attention, response inhibition and brain event-related potential alterations in adults with beta-thalassaemia major. *Br J Haematol* 2019; 186: 580–591.
69. Helfrich RF and Knight RT. Cognitive neurophysiology: event-related potentials. *Handb Clin Neurol* 2019; 160: 543–558.

70. Carlson JM. A systematic review of event-related potentials as outcome measures of attention bias modification. *Psychophysiology* 2021; 58: e13801.
71. de Tommaso M, Betti V, Bocci T, *et al.* Pearls and pitfalls in brain functional analysis by event-related potentials: a narrative review by the Italian Psychophysiology and Cognitive Neuroscience Society on methodological limits and clinical reliability-part I. *Neurol Sci* 2020; 41: 2711–2735.
72. Dessoki HH, Soltan MR and Ezzat AA. Cognitive deficits in patients with  $\beta$ -thalassemia major. *Middle East Current Psychiatry* 2018; 25: 127–130.
73. Wang X, Wang Z, Cao J, *et al.* Ferroptosis mechanisms involved in hippocampal-related diseases. *Int J Mol Sci* 2021; 22: 9902.
74. Bao WD, Pang P, Zhou XT, *et al.* Loss of ferroportin induces memory impairment by promoting ferroptosis in Alzheimer's disease. *Cell Death Differ* 2021; 28: 1548–1562.
75. Badea A, Delpratt NA, Anderson RJ, *et al.* Multivariate MR biomarkers better predict cognitive dysfunction in mouse models of Alzheimer's disease. *Magn Reson Imaging* 2019; 60: 52–67.
76. Ji P, Lönnerdal B, Kim K, *et al.* Iron oversupplementation causes hippocampal iron overloading and impairs social novelty recognition in nursing piglets. *J Nutr* 2019; 149: 398–405.
77. Kalpouzos G, Mangialasche F, Falahati F, *et al.* Contributions of HFE polymorphisms to brain and blood iron load, and their links to cognitive and motor function in healthy adults. *Neuropsychopharmacol Rep* 2021; 41: 393–404.
78. Biel D, Steiger TK and Bunzeck N. Age-related iron accumulation and demyelination in the basal ganglia are closely related to verbal memory and executive functioning. *Sci Rep* 2021; 11: 9438.
79. Gao L, Jiang Z, Cai Z, *et al.* Brain iron deposition analysis using susceptibility weighted imaging and its association with body iron level in patients with mild cognitive impairment. *Mol Med Rep* 2017; 16: 8209–8215.
80. Akhlaghpour S, Ghahari A, Morteza A, *et al.* Quantitative T2\* magnetic resonance imaging for evaluation of iron deposition in the brain of  $\beta$ -thalassemia patients. *Clin Neuroradiol* 2011; 22: 211–217.
81. Qiu D, Chan GC, Chu J, *et al.* MR quantitative susceptibility imaging for the evaluation of iron loading in the brains of patients with  $\beta$ -thalassemia major. *AJNR Am J Neuroradiol* 2014; 35: 1085–1090.
82. Manara R, Ponticorvo S, Tartaglione I, *et al.* Brain iron content in systemic iron overload: a beta-thalassemia quantitative MRI study. *Neuroimage Clin* 2019; 24: 102058.
83. Witzleben CL and Wyatt JP. The effect of long survival on the pathology of thalassaemia major. *J Pathol Bacteriol* 1961; 82: 1–12.

Visit SAGE journals online  
[journals.sagepub.com/  
 home/tah](http://journals.sagepub.com/home/tah)

 SAGE journals